 CMES, vol.95, no.6, pp.501-517, 2013

Numerical Evalution of Eshelby's Tensor of Anisotropic Ferromagnetic Shape Memory Alloy and Its Influence on Magnetic Field-induced Strain

Yuping Zhu[1,2], **Tao Shi**[1] **and Yuanbing Wang**[1]

Abstract: Single crystal ferromagnetic shape memory alloy is a kind of new intelligent materials, it shows obvious anisotropy. Micromechanics theory has been used to analyze the whole mechanical behaviors of this material. However, Eshelby's tensor of this material which plays an important role has still not solved efficiently. Based on the existing micromechanics constitutive model, this paper analyzes the numerical calculation formula of Eshelby's tensor of anisotropic ferromagnetic shape memory alloy. Adopting the way of Gauss integral, the optimal Gaussian integral points for different inclusion shapes and the corresponding numerical solution of Eshelby's tensor are obtained.Furthermore, the influence of inclusion shapes on interaction energy and magnetic field-induced strains of Ni_2MnGa single crystal is analyzed.It shows that the interaction energy of penny inclusion of ferromagnetic shape memory alloy is the maximum. The magnetic field-induced strain of spherical inclusion is the most close to experimental data. The above results can provide theoretical guidance for design and use of ferromagnetic shape memory alloy.

Keywords: Ferromagnetic shape memory alloy, Anisotropy, Eshelby tensor, Numerical calculation.

1 Introduction

In recent years, intelligent materials have been explored deeply [Liu, Dui and Zhu (2011); Xue, Dui and Liu (2013)]. Ni_2MnGa, as the representative of single crystal ferromagnetic shape memory alloy (FSMA) is of intriguing interest of the scholars in many countries [Heczko, Sozinov and Ullakko (2000); Yang (2000)]. FSMA possesses ferromagnetic and shape memory effect. Shape memory effect can be induced by temperature, stress and magnetic field. The magnetic field-induced

[1] Institute of Mechanics & Engineering, Jiangsu University, Zhenjiang 212013, China.
[2] Corresponding author: Tel: +86 511-88780197, E-mail: zhuyuping@126.com

strain of Ni_2MnGa single crystals can reach to 10% [Heczko, Sozinov and Ullakko (2000); Murray, Marioni, Allen, Ohandley and Lograsso (2000)]. As FSMA exports large strain under the active magnetic field with rapid frequency, which makes it possible to the important use in the field of vibration and noise control, micro-displacement machine, microwave devices and intelligent structure, it becomes driving and sensing materials of new generation.

Many scholars have done lots of researches on material preparation, crystal structure, domain evolution, phase transformation characteristic, strain mechanism and mechanical behaviors. As a result, they have made some phased progress[Chen, Tian, Li and Zheng (2007); Karaca, Karaman, Basaran and Lagoudas (2007); Sui, Gao, Yu, Zhang and Cai (2008); Wang, Ren, Nie, Liu, Zuo, Choo, Li, Liaw, Yan, McQueeney, Richardson and Huq (2007)]. Ni_2MnGa belongs to Heuslur alloys, it is first found that it both has ferromagnetism and thermoelastic martensitic phase transformation characteristics. FSMA has rich microstructures, such as magnetocrystalline anisotropy, magnetic domain, magnetic direction, etc. Shape memory effect and super-elastic properties of FSMA have to do with microstructure and magnetomechanics path of the material.

In recent years, there are a lot of literatures on mechanical constitutive relations of FSMA. For example, the models were based on microscopic magnetism [Desimone and James (2002); James and Wuttig (1998)], continuum thermodynamic [Kieer and Lagoudas (2005); Pei and Fang (2007)], statistic mechanics [Glavatska, Rudenko, Glavatskiy and L'vov (2003)], non-equilibrium thermodynamic [Hirsinger and Lexcellent (2003)], micro-mechanics theory and thermodynamic principle [Zhu and Dui (2008)]. Researchers adopted different ways to study mechanical constitutive relations of FSMA from different aspects. However, single crystal ferromagnetic shape memory alloy shows an obvious anisotropy, the above models did not consider material anisotropy, as a result, they could not fully describe the mechanical behaviors of FSMA.

Literatures [Wang, Li and Hu (2012); Zhu and Yu (2013)] considered the magnetic field-induced strain affected by material anisotropy by using micromechanics and thermodynamic principle. In the literature Wang,Li and Hu (2012), it mainly analyzed the magnetic field-induced strain affected by the shape of inclusion, but the analysis and calculation of Eshelby's tensor was not involved. Though literature Zhu and Yu (2013) introduced the numerical calculation of Eshelby's tensor, it only considered the situation of spherical inclusion for simple calculation. However, Eshelby's tensor is important in many semi-analytical micromechanical models, such as self-consistent, mori-tanaka, etc. As we all know, Eshelby's tensor has to do with matrix material properties and the shape of inclusions. FSMA shows obvious anisotropy, its analytical solution of Eshelby's tensor cannot be obtained

[Mura (1987)]. In order to fully predict the behaviors of the FSMA and explore the full engineering potential of FSMA, it is important to deeply analyze the numerical calculation of Eshelby's tensor with different inclusion shapes and its influence on magnetic field-induced strain. Recently, many numerical methods of Eshelby's tensor have been developed for heterogeneous materials [Dong and Atluri (2012a); Dong and Atluri (2012b); Dong and Atluri (2013)].

This paper, based on the present micromechanical model, takes Ni_2MnGa which is the 5M modulation structure into account. First, it analyzes the calculation formula of Eshelby's tensor of anisotropic matrix material. It uses the way of Gauss integral to obtain the optimal Gaussian integration nodes and the arithmetic solution of Eshelby's tensor for different inclusion shapes. Based on the above results, it further analyzes the influence of different inclusion shapes on Ni_2MnGa interaction energy and magnetic field-induced strain.

2 Mechanical constitutive model of Ni_2MnGa

The structure of austenitic parent phase is body-centered cubic in Ni_2MnGa. Martensitic phase is tetragonal structure, it is generally exists three variants, see Fig.1 [Kieer and Lagoudas (2005)]. The magnetic field-induced strain of FSMA is mainly included by three aspects: phase transition from austenitic phase to martensitic phase, magnetostrictive effect and martensite twin reorientation [Kieer and Lagoudas (2005)]. However, the former two ones are relatively smaller than the last one, so the magnetic field-induced strain induced by martensite twin reorientation in FSMA is only considered in this paper.

It is supposed that the material initial situation is full martensite. Variant 1 can be obtained by single axial stress σ^0.When magnetic field $\mathbf{H}$ which is perpendicular to σ^0 is applied, if magneto crystalline anisotropy energy is more than that of detwinning, the direction of twin crystal may turn into another one, variant 2 is produced and twin boundaries begin to move, then the strain is induced, see Fig. 2. When magnetic field decreases or it disappears, the twin boundaries return to the initial situation and the material returns to the initial shape. This is the shape memory effect.

When we apply stress coupling with magnetic field, it exists two martensitic variants and two magnetic domains, see Fig. 3 [Kieer and Lagoudas (2005)]. The easy axis direction of variant 1 is along x-axis, the easy axis direction of variant 2 is along $y-$axis. The magnetization direction of magnetic domain 1 is the negative of x-axis, the magnetization direction of magnetic domain 2 is x-axis, the dashed lines in the figure represent the initial structure of magnetization vector. In the process of microscopic structure evolution, we choose reorientation strain ε^{tr}, the

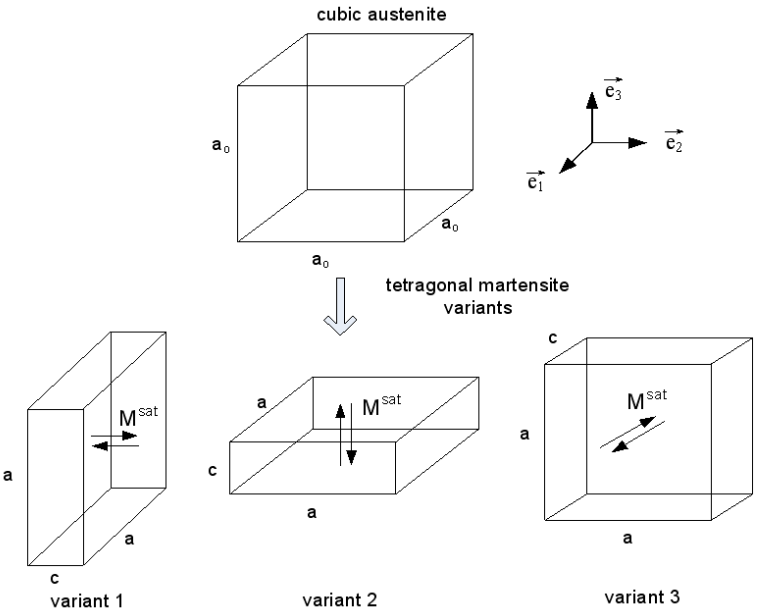

Figure 1: Crystal structure of the austenitic phase and the martensite variants in Ni_2MnGa [Kieer and Lagoudas (2005)]

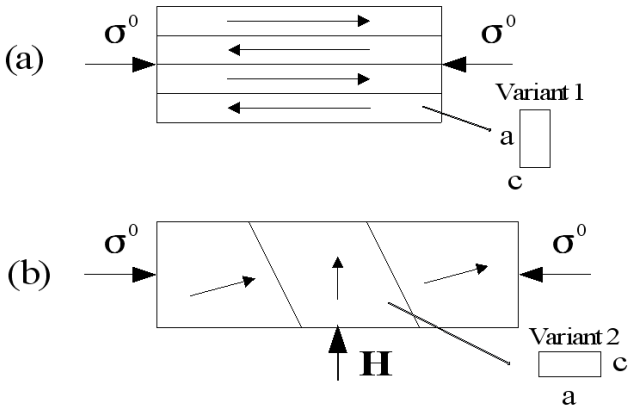

Figure 2: Schematic of a FSAM single-crystal specimen under field and stress [Kieer and Lagoudas (2005); Zhu and Dui(2008)]

volume fraction ξ of variant 2, the volume fraction α of magnetic domain 2, the intersection angle which is relative to the initial situation of magnetization vector β_i (i=1,2,3,4) as the appropriate sets of internal state variables.

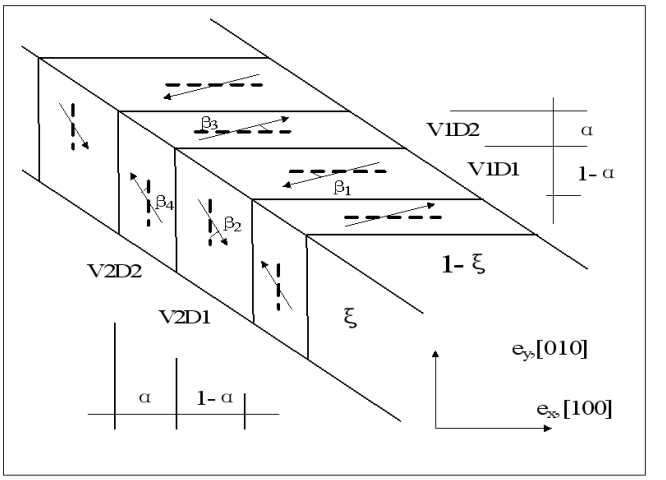

Figure 3: Schematic of a twin boundary during the reorientation process of FSMA[Kieer and Lagoudas(2005)]

2.1 Micromechanics constitutive model

This paper is based on the constitutive model of literatures [Zhu and Dui (2008); Zhu and Yu (2013)], the constitutive model is explained as follow.

FSMA is regarded as a two-phase system, variant 1 is matrix phase, variant 2 is inclusion phase. When the material is applied the stress of homogeneous state, we assume $\bar{\mathbf{M}}$ as the effective elastic compliance tensor, $\bar{\varepsilon}$ as the average strain, $\bar{\varepsilon}^{in}$ as the inelastic strain, it exists as follow.

$$\bar{\boldsymbol{\varepsilon}} - \bar{\boldsymbol{\varepsilon}}^{in} = \bar{\mathbf{M}}\boldsymbol{\sigma}^0 \tag{1}$$

When it has no inclusion, applied the same stress, then

$$\boldsymbol{\sigma}^0 = \mathbf{C}_0\boldsymbol{\varepsilon}^0 \tag{2}$$

where $\mathbf{C}_0$ is the elastic stiffness tensor of matrix material.

When the inclusion is produced, as a result, disturbed stress $\tilde{\boldsymbol{\sigma}}$ and disturbed strain $\tilde{\boldsymbol{\varepsilon}}$ are produced, the average stress in the matrix is as follow.

$$\boldsymbol{\sigma}^{(0)} = \boldsymbol{\sigma}^0 + \tilde{\boldsymbol{\sigma}} = \mathbf{C}_0(\boldsymbol{\varepsilon}^0 + \tilde{\boldsymbol{\varepsilon}}) \tag{3}$$

We choose $\boldsymbol{\varepsilon}^{'}$ as the strain difference between inclusion phase and matrix phase. The stress in inclusion through the Eshelby equivalent inclusion principle is

$$\boldsymbol{\sigma}^{(1)} = \mathbf{C}_1(\boldsymbol{\varepsilon}^0 + \tilde{\boldsymbol{\varepsilon}} + \boldsymbol{\varepsilon}^{'} - \boldsymbol{\varepsilon}^{tr}) = \mathbf{C}_0(\boldsymbol{\varepsilon}^0 + \tilde{\boldsymbol{\varepsilon}} + \boldsymbol{\varepsilon}^{'} - \boldsymbol{\varepsilon}^{tr} - \boldsymbol{\varepsilon}^{*}) \tag{4}$$

where ε^{tr} represents the reorientation strain, $\mathbf{C}_1, \boldsymbol{\varepsilon}^{*}$ represent the elastic stiffness tensor of inclusion and the equivalent intrinsic strain, as a result

$$\boldsymbol{\varepsilon}^{'} = \mathbf{S}(\boldsymbol{\varepsilon}^{tr} + \boldsymbol{\varepsilon}^{*}) \tag{5}$$

where $\mathbf{S}$ is Eshelby's tensor, it has something to do with the material property of variant 1 and the shape of variant 2. As the whole volume average stress is equal to the average stress of boundary, we can obtain the macro-average strain of FSMA through the Eqs.(2) to (5).

$$\begin{aligned}\bar{\boldsymbol{\varepsilon}} =& [\mathbf{I} + \xi\{\mathbf{C}_0 + (\mathbf{C}_1 - \mathbf{C}_0)[\mathbf{S} - \xi(\mathbf{S} - \mathbf{I})]\}^{-1}(\mathbf{C}_0 - \mathbf{C}_1)]\mathbf{C}_0^{-1}\boldsymbol{\sigma}^0 + \xi\boldsymbol{\varepsilon}^{tr} \\ &+ \xi(1-\xi)\{\mathbf{C}_0 + (\mathbf{C}_1 - \mathbf{C}_0)[\mathbf{S} - \xi(\mathbf{S} - \mathbf{I})]\}^{-1}(\mathbf{C}_0 - \mathbf{C}_1)(\mathbf{S} - \mathbf{I})\boldsymbol{\varepsilon}^{tr}\end{aligned} \tag{6}$$

where $\mathbf{I}$ is the four order equivalent tensor, ξ represents the volume fraction of variant 2 and it has something to do with temperature, stress field and magnetic field.

2.2 Variant reorientation thermodynamic criterion

We assume that there is no change of entropy in the process of variant reorientation, Gibbs free energy mainly includes three parts: mechanical potential energy G_{me}, Zeeman free energy G_{Zee}, magnetocrystalline anisotropy energy G_{an} and other energy is ignored. The Gibbs free energy of per unit volume is

$$G(\boldsymbol{\sigma}^0, T, \xi) = G_{me}(\boldsymbol{\sigma}^0, T, \xi) + G_{Zee}(\mathbf{H}, \mathbf{M}, \xi, \alpha) + G_{an}(\alpha, \beta_i) \tag{7}$$

where T represents absolute temperature, $\mathbf{H}$ represents magnetic field intensity, $\mathbf{M}$ represents magnetization.

If the material has no other inclusion and the boundary is applied the force of $\mathbf{F}$, the corresponding displacement, stress and elastic strain are represented by $\mathbf{u}^0$, $\boldsymbol{\sigma}^0$ and $\boldsymbol{\varepsilon}^0$, as it has non-homogeneous inclusion, the corresponding displacement, stress and strain are represented by $\mathbf{u}^0 + \mathbf{u}$, $\boldsymbol{\sigma}^0 + \boldsymbol{\sigma}$ and $\boldsymbol{\varepsilon}^0 + \boldsymbol{\varepsilon}$, mechanical potential energy of the material is [Mura (1987); Zhu and Yu (2013)]

$$\begin{aligned}G_{me} =& -\frac{1}{2}\xi\{\mathbf{C}_0(\mathbf{S} - \mathbf{I})\boldsymbol{\varepsilon}^{tr}\boldsymbol{\varepsilon}^{tr} + 2\boldsymbol{\sigma}^0\boldsymbol{\varepsilon}^{tr} - \boldsymbol{\sigma}^0[(\mathbf{C}_1 - \mathbf{C}_0)\mathbf{S} + \mathbf{C}_0]^{-1}(\mathbf{C}_1 - \mathbf{C}_0)\boldsymbol{\varepsilon}^0 \\ &- \mathbf{C}_0(\mathbf{S} - \mathbf{I})[(\mathbf{C}_1 - \mathbf{C}_0)\mathbf{S} + \mathbf{C}_0]^{-1}(\mathbf{C}_1 - \mathbf{C}_0)\boldsymbol{\varepsilon}^0\boldsymbol{\varepsilon}^{tr}\} + G_{me}^0\end{aligned}$$

(8)

where G^0_{me} represents the initial mechanical potential energy. Through the definition of interaction energy in literature [Mura (1987)], we can get the interaction energy of anisotropic material.

$$\begin{aligned} W_{int} = &-\frac{1}{2}\xi\{\mathbf{C}_0(\mathbf{S}-\mathbf{I})\boldsymbol{\varepsilon}^{tr}\boldsymbol{\varepsilon}^{tr} + 2\boldsymbol{\sigma}^0\boldsymbol{\varepsilon}^{tr} - \boldsymbol{\sigma}^0[(\mathbf{C}_1-\mathbf{C}_0)\mathbf{S}+\mathbf{C}_0]^{-1}(\mathbf{C}_1-\mathbf{C}_0)\boldsymbol{\varepsilon}^0 \\ &-\mathbf{C}_0(\mathbf{S}-\mathbf{I})[(\mathbf{C}_1-\mathbf{C}_0)\mathbf{S}+\mathbf{C}_0]^{-1}(\mathbf{C}_1-\mathbf{C}_0)\boldsymbol{\varepsilon}^0\boldsymbol{\varepsilon}^{tr}\} \end{aligned} \tag{9}$$

The magnetic intensity vector which is along y-axis can be showed as follow.

$$\mathbf{H} = H\mathbf{e}_y \tag{10}$$

where $\mathbf{e}_y$ represents the axis unit vector.

Under the magnetic field, for simple calculation, we assume the material has only one fixed magnetic domain and α equals to 1. The result derived from the model is consistent with the experimental data [Kieer and Lagoudas (2005)]. With the increase of magnetic field, as the direction of magnetization vector of variant 2 is along the direction of magnetic field, so $\beta_4 = 0$. The Zeeman free energy is showed as follow [Kieer and Lagoudas (2005); Zhong (1987)].

$$G_{Zee} = -\mu_0\mathbf{H}\cdot\mathbf{M} = -\mu_0 M^{sat} H[(1-\xi)\sin\beta_3 + \xi] \tag{11}$$

where M^{sat} represents saturation magnetization .

Through the literatures [Kieer and Lagoudas (2005); Zhong (1987)], the magneto crystalline anisotropy energy of FSMA is

$$G_{an} = K_u(1-\xi)\sin^2\beta_3 \tag{12}$$

where K_u is the magnetic anisotropy constant. We take the moment without magnetic field as the initial state, the change of Zeeman free energy is ΔG

$$\Delta G(\boldsymbol{\sigma}^0, T, \xi, \alpha) = W_{int} - \mu_0\mathbf{H}\cdot\mathbf{M} + G_{an} \tag{13}$$

ΔG offers the phase transition drive force for orientation of martensitic variants.

$$f_{drv} = -\frac{\partial\Delta G}{\partial\xi} = -\frac{\partial W_{int}}{\partial\xi} + \frac{\partial}{\partial\xi}(\mu_0\mathbf{H}\cdot\mathbf{M}) - \frac{\partial G_{an}}{\partial\xi} \tag{14}$$

The resistance of martensitic variants reorientation mainly includes: interface energy and dissipation of energy induced by twin boundary surface movement. We choose γ_s as surface energy density and t as the average thickness of variant 2.The

surface energy variable of per unit volume ΔG_s is [Zhu and Dui (2008); Zhu and Yu (2013)]

$$\Delta G_s = 2\xi\gamma_s/t \tag{15}$$

For FSMA, through the experimental data, the dissipation of energy is showed as the follow empirical formula [Zhu and Yu (2013)]

$$\Delta G_d = D(e^{b\xi} - 1) \tag{16}$$

where D and b are undetermined material constants, then the resistance of martensitic variants reorientation is as follow.

$$f_{res} = \frac{\partial}{\partial\xi}(\Delta G_s + \Delta G_d) = 2\gamma_s/t + Dbe^{b\xi} \tag{17}$$

At the time of equilibrium state of variant reorientation, the kinetic equation of martensitic variants reorientation is [Zhu and Yu (2013)]

$$\begin{aligned}&\frac{1}{2}\{\mathbf{C}_0(\mathbf{S}-\mathbf{I})\boldsymbol{\varepsilon}^{tr}\boldsymbol{\varepsilon}^{tr} + 2\boldsymbol{\sigma}^0\boldsymbol{\varepsilon}^{tr} - \boldsymbol{\sigma}^0[(\mathbf{C}_1-\mathbf{C}_0)\mathbf{S}+\mathbf{C}_0]^{-1}(\mathbf{C}_1-\mathbf{C}_0)\boldsymbol{\varepsilon}^0\\ &-\mathbf{C}_0(\mathbf{S}-\mathbf{I})[(\mathbf{C}_1-\mathbf{C}_0)\mathbf{S}+\mathbf{C}_0]^{-1}(\mathbf{C}_1-\mathbf{C}_0)\boldsymbol{\varepsilon}^0\boldsymbol{\varepsilon}^{tr}\}\\ &+K_u\sin^2\beta_3 + \mu_0 M^{sat}H(1-\sin\beta_3) = 2\gamma_s/t + Dbe^{b\xi}\end{aligned} \tag{18}$$

When the external force and magnetic field intensity are set, we can obtain the volume fraction of variant 2 through the above equations. Then we can obtain the macro-strain through Eq. (6). Similarity, when the external force or magnetic field decreases, variant 2 would turn into variant 1, called inverse reorientation.Respectively, we can choose variant 2 as matrix and variant 1 as inclusion, then get the volume fraction of the inclusion.

3 Numerical calculation of Eshelby's Tensor

Under the uniform field, the elastic field is also uniform in ellipsoidal inclusion. Eshelby's tensor has something to do with the property of matrix material and the shape of inclusion. It has the form of ellipsoid integral. For anisotropic material, Eshelby's tensor has no analytic solution [Eshelby (1957); Mura (1987)].Through the Eqs.(6) and (18), for FSMA, both the micromechanics constitutive model and the reorientation thermodynamic criterion have something to do with the Eshelby's tensor. In order to analyze the macroscopic mechanical behaviors of single crystal FSMA, we should first analyze the analytic solution of Eshelby's tensor.

Eshelby's tensor is a fourth-order tensor, for general anisotropic matrix material, Eshelby's tensor has the form as follow [Gavazzi and Lagoudas (1990)].

$$S_{ijkl} = \frac{1}{8\pi} C^0_{ijkl} \int_{-1}^{+1} d\xi_3 \int_0^{2\pi} \{G_{imjn}(\bar{\xi}) + G_{jmin}(\bar{\xi})\} d\omega \tag{19}$$

where

$$\begin{aligned} &G_{imjn}(\bar{\xi}) = \bar{\xi}_k \bar{\xi}_l N_{ij}(\bar{\xi}) / D(\bar{\xi}) \\ &\bar{\xi}_i = \zeta_i / a_i \quad \zeta_1 = (1-\zeta_3^2)^{1/2} \cos\omega \quad \zeta_2 = (1-\zeta_3^2)^{1/2} \sin\omega \quad \zeta_3 = \zeta_3 \\ &D(\bar{\xi}) = d_{mnl} K_{m1} K_{n2} K_{l3} \quad N_{ij}(\bar{\xi}) = \frac{1}{2} d_{ikl} d_{jmn} K_{km} K_{\ln} \quad K_{ik} = C^0_{ijkl} \bar{\xi}_j \bar{\xi}_l \end{aligned} \tag{20}$$

where d_{ijk} is a permutation tensor, a_i(i=1,2,3) is the principal axis of ellipsoid, the double integral of Eq.(20) can be showed as the following Gaussian integral formula [Gavazzi and Lagoudas (1990)].

$$S_{ijkl} = \frac{1}{8\pi} \sum_{p=1}^{M} \sum_{q=1}^{N} C^0_{mnkl} \{G_{imjn}(\omega_q, \zeta_{3p}) + G_{jmin}(\omega_q, \zeta_{3p})\} W_{pq} \tag{21}$$

where M and N refer to the integral point of ζ_3 and ω_q respectively, W_{pq} is Gaussian weight.

Through a series of analysis and calculation, the optimal M and N of inclusions of different shapes are determined . For checking the accuracy of the numerical results, each kind of inclusion shapes degenerates into isotropy respectively. And we compare the results with the analytical solution of isotropy matrix, the error of the nonzero term of Eshelby's tensor is not more than five percent.

We assume that the direction of the initial variant 1 is along that of crystal axises, martensite variant 1 has 6 independent material constants [Dai, Cui and Wuttig (2003)], namely, C_{11}=39GPa, C_{12}=30GPa, C_{13}=27.6GPa, C_{33}=28GPa, C_{44}=51GPa, C_{66}=49GPa.

In the process of the transform from variant 1 to variant 2, we can obtain elastic stiffness matrix by rotation tensor which is applied to the reference state [Zhu and Yu(2013)].

$$C^1_{ijks} = a_{ip} a_{jq} a_{kr} a_{st} C^0_{pqrs} \tag{22}$$

where a_{mn} stands for the component of transfer matrix which is relative to crystal reference frame.

For single crystal FSMA, we consider some kinds of inclusion shapes, the numerical solution of Eshelby's tensor is as follow.

For spherical inclusion, in Eq.(20), a_1=a_2=a_3=3, M=N=40, the nonzero terms of Eshelby's tensor are as follows.

$$\mathbf{S}=\begin{bmatrix} 0.3372 & 0.1238 & 0.1403 & & & & \\ 0.1240 & 0.3375 & 0.1405 & 0 & & & \\ 0.1673 & 0.1673 & 0.2801 & & & & \\ & & & 0.3420 & & & \\ & 0 & & & 0.3429 & & \\ & & & & & 0.3386 & \end{bmatrix} \tag{23}$$

For oblate spheroid inclusion, in Eq.(20), $a_1 = a_2$=3, a_3=12, $M = N$=1000, the nonzero terms of Eshelby's tensor are as follows.

$$\mathbf{S}=\begin{bmatrix} 0.5115 & 0.1899 & 0.2698 & & & & \\ 0.1899 & 0.5115 & 0.2698 & 0 & & & \\ -0.0091 & -0.0091 & 0.1766 & & & & \\ & & & 0.2836 & & & \\ & 0 & & & 0.2836 & & \\ & & & & & 0.4126 & \end{bmatrix} \tag{24}$$

For penny inclusion, in Eq.(20), a_1=a_2=300, a_3=1, M=N=1000, the nonzero terms of Eshelby's tensor are as follows.

$$\mathbf{S}=\begin{bmatrix} 0.0008 & -0.0004 & -0.0006 & & & & \\ -0.0004 & 0.0008 & -0.0006 & 0 & & & \\ 0.9822 & 0.9822 & 0.9982 & & & & \\ & & & 0.4985 & & & \\ & 0 & & & 0.4985 & & \\ & & & & & 0.0029 & \end{bmatrix} \tag{25}$$

For elliptic cylinder inclusion, in Eq.(20), a_1=a_2=3, a_3=300, M=N=1000, the nonzero terms of Eshelby's tensor are as follows.

$$\mathbf{S}=\begin{bmatrix} 0.5630 & 0.1766 & 0.2958 & & & & \\ 0.1766 & 0.5630 & 0.2958 & 0 & & & \\ -0.0002 & -0.0002 & -0.0001 & & & & \\ & & & 0.2503 & & & \\ & 0 & & & 0.2503 & & \\ & & & & & 0.4363 & \end{bmatrix} \tag{26}$$

4 Numerical calculation and results

4.1 The influence of inclusion shapes on interaction energy

Interaction energy is a rather important part of elastic strain energy, which has to do with phase transition and variant reorientation. It embodies interaction effect among inclusion, eigenstrain and matrix. Though the energy is relatively small, it plays an assignable part in the form of hysteresis characteristic of FSMA. In reference [Zhu and Yu (2013)], it plots the interaction energy vs. volume fraction of variant 2 under different compressive stresses with spherical inclusion. However, the effect of the inclusion shapes is not considered. Based on Eq. (9), this paper focuses on analyzing the influence of inclusion shapes on the interaction energy of FSMA.

It is supposed that the single axial stress is as follow.

$$[\boldsymbol{\sigma}^0] = \begin{bmatrix} \sigma & 0 & 0 \\ 0 & 0 & 0 \\ 0 & 0 & 0 \end{bmatrix} \tag{27}$$

where $\boldsymbol{\sigma}$ is a constant.

The component of the external magnetic field $\mathbf{H}$ is as follow.

$$[\mathbf{H}] = \begin{bmatrix} 0 \\ H \\ 0 \end{bmatrix} \quad H > 0 \tag{28}$$

Under magnetic field and stress, the reorientation strain is along axis, the relative expression is as follow.

$$[\boldsymbol{\varepsilon}^{tr}] = \varepsilon^{r,\max} \begin{bmatrix} 1 & 0 & 0 \\ 0 & -1 & 0 \\ 0 & 0 & 0 \end{bmatrix} \tag{29}$$

where $\varepsilon^{r,\max}$ is the maximum reorientation strain, which is determined by experiments. The material constants of single crystal $Ni_{49}Mn_{29}Ga_{22}$ under 0.1MPa compressive stress are showed in table 1 [Bechtold, Gerber,Wuttig and Quandt (2008)]. The critical value $\mu_0 H^{s(1,2)}$ respects the magnetic field which is at the beginning of the process of the reorientation from variant 1 to variant 2, the critical value $\mu_0 H^{f(1,2)}$ means the magnetic field which is at the end of the process of the reorientation from variant 1 to variant 2. $\mu_0 H^{s(2,1)}$, $\mu_0 H^{f(2,1)}$ respects the beginning critical magnetic field and the final critical magnetic field from variant 2 to variant 1, respectively.

Table 1: Material constants and critical field for a Ni_2MnGa specimen [Bechtold, Gerber,Wuttig and Quandt (2008)]

Quantity	Value(unit)	Quantity	Value(unit)
μ_0	1.256 μNA^{-2}	$\mu_0 H^{s(1,2)}$	0.2T
M^{sat}	500 kAm^{-1}	$\mu_0 H^{f(1,2)}$	0.84T
K_u	2.1×10^5J/m^3	$\mu_0 H^{s(2,1)}$	0.49T
$\varepsilon^{r,max}$	0.055	$\mu_0 H^{f(2,1)}$	-0.25T

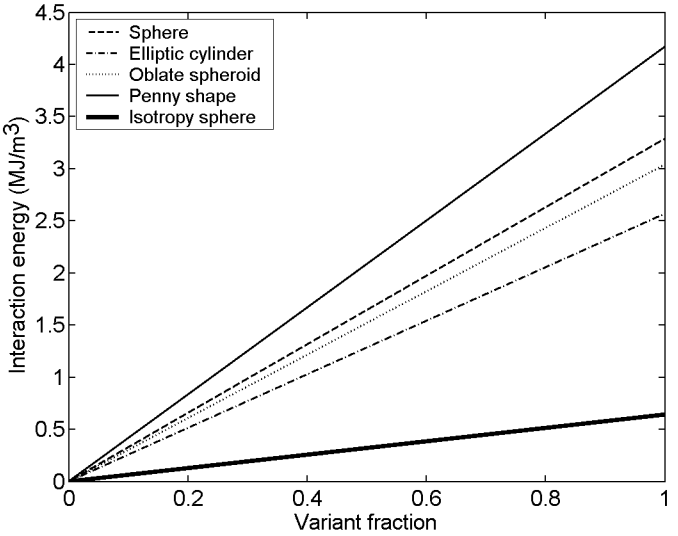

Figure 4: Interaction energy vs.variant 2 volume fraction of FSMA with different inclusion shapes

Under -1MPa compressive stress, the interaction energy of FSMA changes as a function of the volume fraction with different inclusion shapes, see Fig. 4. The thick solid line represents the case of isotropic spherical inclusion, the thin solid line represents penny inclusion with anisotropic matrix, the dashed line represents the case of anisotropic spherical inclusion, the dotted line represents the case of anisotropic oblate spheroid inclusion and the dash-dotted line represents the case of anisotropic elliptic cylinder inclusion. As seen in Fig.4, the interaction energy of FSMA is different with different inclusion shapes. It shows linear change with the volume fractions of variant 2. For anisotropic matrix, the interaction energy of

penny inclusion reaches to the maximum value, the spherical inclusion takes the second place, the elliptic cylinder inclusion takes the last place, the case of oblate spheroid inclusion is between the spherical inclusion and elliptic cylinder inclusion, and the case of isotropic spherical inclusion is less than that of anisotropic matrix.

4.2 The influence of inclusion shapes on macroscopic strain of FSMA

For FSMA, magnetization vectors angle is dependent on the minimum energy principle under magnetic field [Cullity (1972)].

$$\frac{\partial \Delta G}{\partial \beta_3} = 0 \tag{30}$$

The rotation angle of magnetization vector β_3 is showed as follow [Zhu and Dui (2008); Zhu and Yu (2013)]

$$\sin\beta_3 = \frac{\mu_0 M^{sat}}{2K_u} H \tag{31}$$

As $0 \leq \beta_3 \leq 90^0$, namely, $0 \leq \sin\beta_3 \leq 1$, the restricted condition of magnetic field can be obtained through Eq.(31).

$$0 \leq \mu_0 H \leq \frac{2K_u}{M^{sat}} \tag{32}$$

The critical magnetic field needed for full reorientation of variant 1 is as follow [Zhu and Dui (2008); Zhu and Yu (2013)]

$$\mu_0 H^{thre} = \frac{2K_u}{M^{sat}} \tag{33}$$

From the above analysis, when the magnetic field intensity is equal to $\mu_0 H^{thre}$, the rotation angle $\beta_3 = 90^\circ$. At this moment, the magnetization vector of variant 1 is along the external magnetic field. With the increase of magnetic field intensity, $\sin\beta_3 \equiv 1$, it remains the same. Through Eq.(18), when the magnetic field intensity is equal to $\mu_0 H^{thre}$, the increase of magnetic field intensity has no effect on kinetic equation and it cannot increase phase transition drive force. As a result, if $\mu_0 H^{f(1,2)} > \mu_0 H^{thre}$, variant 1 can't fully turn into variant 2. On the contrary, if $\mu_0 H^{f(1,2)} \leq \mu_0 H^{thre}$, variant 1 can fully turn into variant 2. On the basis of Eq.(33) and table 1, the extreme magnetic field intensity is obtained as $\mu_0 H^{thre} = 0.84T$. So under -0.1MPa compressive stress,variant 1 can fully turn into variant 2. In the process of the reorientation from variant 1 to variant 2, under compressive stress -0.1MPa, we choose b=0.21.Then based on the critical magnetic field intensity $\mu_0 H^{s(1,2)}$, $\mu_0 H^{f(1,2)}$through the Eq.(18), the material constants γ_s/t and D can

be obtained with spherical inclusion. Similarly, for the case of inverse orientation, b=0.62. Based on the critical magnetic field intensity $\mu_0 H^{s(2,1)}$, $\mu_0 H^{f(2,1)}$, through the Eqs.(18) and (31), the relative material constants $\gamma_s/t$and Dcan be solved. Then the kinetic equation of orientation of martensitic variants is obtained. The material constants remain the same, we can predict other strain curves by using Eq.(18) to Eq.(31).

The computed magnetic field vs. strain curves with different inclusion shapes of anisotropic matrix under different -1.2MPa compressive stresses are displayed in Fig. 5. The vertical axis represents orientation strain. The thin solid line represents experimental data [Bechtold, Gerber, Wuttig and Quandt (2008)], the dotted line represents spherical inclusion, the dashed line represents oblate spheroid inclusion, the thick solid line represents elliptic cylinder inclusion, and the dash-dotted line represents penny inclusion. As seen in Fig. 5, strain of spherical inclusion is most close to the experimental data. The strain of elliptic cylinder is relatively close to that of penny inclusion and the result is smaller than that of experiment.

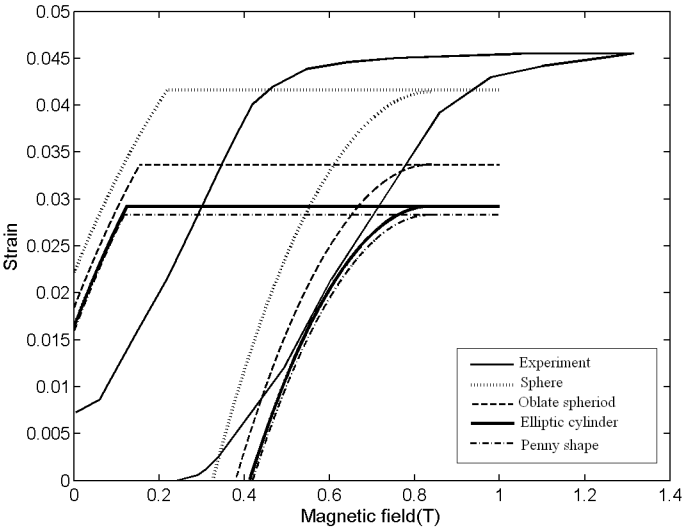

Figure 5: Magnetic field vs. strain curves with different inclusion shapes

5 Conclusions

Based on the existing micro-mechanics constitutive model, this paper analyzes the formula of Eshelby's tensor of anisotropic ferromagnetic shape memory alloy.

It adopts the way of Gaussian integral and obtains the optimal Gaussian integral points of different inclusions shapes. In addition, arithmetic solution of Eshelby's tensor with different inclusion shapes is also obtained. Based on the above results, it deeply analyses the influence of different inclusion shapes on the interaction energy and the magneto-strain of Ni_2MnGa. By comparing the results, the interaction energy of FSMA changes linearly with the volume fraction of variant 2 with different inclusion shapes. The interaction energy of penny inclusion in anisotropic matrix is the maximum; the result of elliptic cylinder inclusion is the minimum. The magneto-strain of spherical inclusion is most close to experimental data. All these conclusions offer theory basis for the design and use of FSMA.

Acknowledgement: The authors acknowledge the financial support of National Science Foundation of China (Nos. 11272136,10972027) and the Foundation of Jiangsu University (No.11JDG066).

References

Bechtold, C.; Gerber, A.; Wuttig, M.; Quandt, E. (2008): Magnetoelastic hysteresis in 5 M NiMnGa single crystals. *Scripta Materialia*, vol. 58, pp. 1022–1024.

Chen, F.; Tian, B.; Li, L.; Zheng, Y. F. (2007): Phase transformation and microstructure of Ni–Mn–Ga ferromagnetic shape memory alloy particles. *Physica Scripta*, vol. T129, pp.227- 230.

Cullity, B. D. (1972): Introduction to Magnetic Materials. Addison-Wesley, Reading: M A.

Dai, L.; Cui, J.; Wuttig, M. (2003): Elasticity of Austenitic and Martensitic NiMnGa. *Proceedings of the Society of Photo-Optical Instrumentation*, vol. 5053, pp.595-602.

Desimone, A.; James, R. (2002): A constrained theory of magnetoelasticity. *Journal of the Mechanics and Physics of Solids*, vol. 50, pp. 283-320.

Dong, L.; Atluri, S. N. (2012a): Development of 3D T-Trefftz voronoi cell finite elements with/without spherical voids &/or elastic/rigid inclusions for micromechanical modeling of heterogeneous materials. *Computers, Materials & Continua*, vol.29, pp.169-212.

Dong, L.; Atluri, S. N. (2012b): T-Trefftz voronoi cell finite elements with elastic/rigid inclusions or voids for micromechanical analysis of composite and porous materials. *Computer Modeling in Engineering & Sciences* , vol.83, pp.183-219.

Dong, L.; Atluri, S. N. (2013): SGBEM Voronoi Cells (SVCs), with embedded arbitrary-shaped inclusions, voids, and/or cracks, for micromechanical modeling of

heterogeneous materials. *Computers, Materials & Continua*, vol.33, pp.111-154.

Eshelby, J. D. (1957): The determination of the elastic field of an ellipsoidal inclusion and related problems. *Proceedings of the Royal Society A*, vol.241, pp.376–396.

Gavazzi, A. C.; Lagoudas, D. C. (1990): On the numerical evaluation of Eshelby's tensor and its application to elastoplastic fibrous composites. *Computational Mechanics*, vol.7, pp.13-19.

Glavatska, N. I.; Rudenko, A. A.; Glavatskiy, I. N.; L'vov, V. A. (2003): Statistical model of magneto- strain effect in martensite. *Journal of Magnetism and Magnetic Materials*, vol.265, pp.142-151.

Heczko, O.; Sozinov, A.; Ullakko, K. (2000): Giant field-induced reversible strain in magnetic shape memory NiMnGa alloy. *IEEE Transactions on Magnetics*, vol.36, pp.3266-3273.

Hirsinger, L.; Lexcellent, C. (2003): Modelling detwinning of martensite platelets under magnetic and (or) stress actions on Ni–Mn–Ga alloys. *Journal of Magnetism and Magnetic Materials*, vol.254-255,pp.275-277.

James, R. D.; Wuttig, M. (1998): Magnetostriction of martensite. *Philosophical Magazine A*, vol.77, pp.1273-1299.

Karaca, H. E.; Karaman, I.; Basaran, B.; Lagoudas, D. C. (2007): On the stress-assisted magne- tic-field-induced phase transformation in Ni_2MnGa ferromagnetic shape memory alloys. *Acta Materialia*, vol.55, pp.4253-4269.

Kieer, B.; Lagoudas, D. C. (2005): Magnetic field-induced martensitic variant reorientation in magnetic shape memory alloys. *Philosophical Magazine*, vol.85, pp. 4289- 4329.

Liu, B. F.; Dui, G. S.; Zhu, Y. P. (2011): A Constitutive Model for Porous Shape Memory Alloys Considering the Effect of Hydrostatic Stress. *Computer Modeling in Engineering & Sciences*, vol.78, pp. 247-275.

Murray, S. J.; Marioni, M.; Allen, S. M.; OHandley, R. C.; Lograsso, T. A. (2000): 6% magnetic- field- induced strain by twin-boundary motion in ferromagnetic Ni-Mn-Ga. *Applied Physics Letters*, vol.77, pp. 886-893.

Mura, T. (1987): Micromechanics of Defects in Solids, Dordrecht etc.. *Martinus Nijhoff Publishers*.

Pei, Y. M.; Fang, D. N. (2007): A model for giant magnetostrain and magnetization in the martensitic phase of NiMnGa alloys. *Smart Materials and Structures*, vol.16, pp.779 -783.

Sui, J.; Gao, Z.; Yu, H.; Zhang, Z. G.; Cai, W. (2008): Martensitic and magnetic transformations of $Ni_{56}Fe_{17}Ga_{27-x}Co_x$ high-temperature ferromagnetic shape

memory alloys. *Scripta Materialia*, vol.59, pp.874-877.

Wang, X.; Li, F.; Hu, Q. (2012): An anisotropic micromechanical-based model for characterizing the magneto-mechanical behavior of NiMnGa alloys. *Smart Materials and Structures*, vol.21, pp. 065021.

Wang, Y. D.; Ren, Y.; Nie, Z. H.; Liu, D. M.; Zuo, L.; Choo, H.; Li, H.; Liaw, P. K.; Yan, J. Q.; McQueeney, R. J.; Richardson, J. W.; Huq, A. (2007): Structural transition of ferromagnetic Ni_2MnGa nanoparticles. *Journal of Applied Physics*, vol.101, pp. 063530.

Xue, L.; Dui, G.; Liu, B. (2013): Theoretical Analysis of a Functionally Graded Shape Memory Alloy Beam under Pure Bending. *Computer Modeling in Engineering & Sciences*, vol.93, pp.1-16.

Yang, D. Z. (2000): Smart Materials and System, Tianjin. *Tianjin University Press* (in Chinese).

Zhong, W. D. (1987): Ferromagnetics, Beijing. *Science Press* (in Chinese).

Zhu, Y. P.; Dui, G. S. (2008): Model for field-induced reorientation strain in magnetic shape memory alloy with tensile and compressive loads. *Journal of Alloys and Compounds*, vol.459, pp.55-60.

Zhu, Y. P.; Yu, K. (2013): Anisotropic modeling of magnetic-field-induced superelastic strain in magnetic shape memory alloy. *Journal of Alloys and Compounds*, vol.550, pp.308-313.